

Proteins in Human Brain Cortex Are Modified by Oxidation, Glycooxidation, and Lipoxidation

EFFECTS OF ALZHEIMER DISEASE AND IDENTIFICATION OF LIPOXIDATION TARGETS*

Received for publication, February 28, 2005, and in revised form, March 25, 2005
Published, JBC Papers in Press, March 29, 2005, DOI 10.1074/jbc.M502255200

Reinald Pamplona^{‡§}, Esther Dalfó^{§¶}, Victòria Ayala[‡], Maria Josep Bellmunt[‡], Joan Prat[‡],
Isidre Ferrer^{¶||}, and Manuel Portero-Otín^{‡**}

From the [‡]Metabolic Pathophysiology Research Group, Departament de Ciències Mèdiques Bàsiques, Facultat de Medicina i Ciències de la Salut, Universitat de Lleida, c/Montserrat Roig, 2, E-25008 Lleida, Spain, the [¶]Institut de Neuropatologia, Servei Anatomia Patològica, Hospital Universitari de Bellvitge, c/Feixa Llarga sn, E-08907, Hospitalet de Llobregat, Barcelona, Spain, and the ^{||}Departament de Biologia Cel·lular i Anatomia Patològica, Facultat de Medicina, Universitat de Barcelona, c/Feixa Llarga sn, E-08907, Hospitalet de Llobregat, Barcelona, Spain

Diverse oxidative pathways, such as direct oxidation of amino acids, glycooxidation, and lipoxidation could contribute to Alzheimer disease pathogenesis. A global survey for the amount of structurally characterized probes for these reactions is lacking and could overcome the lack of specificity derived from measurement of 2,4-dinitrophenylhydrazine reactive carbonyls. Consequently we analyzed (i) the presence and concentrations of glutamic and amino adipic semialdehydes, *N*^ε-(carboxymethyl)-lysine, *N*^ε-(carboxyethyl)-lysine, and *N*^ε-(malondialdehyde)-lysine by means of gas chromatography/mass spectrometry, (ii) the biological response through expression of the receptor for advanced glycation end products, (iii) the fatty acid composition in brain samples from Alzheimer disease patients and age-matched controls, and (iv) the targets of *N*^ε-(malondialdehyde)-lysine formation in brain cortex by proteomic techniques. Alzheimer disease was associated with significant, although heterogeneous, increases in the concentrations of all evaluated markers. Alzheimer disease samples presented increases in expression of the receptor for advanced glycation end products with high molecular heterogeneity. Samples from Alzheimer disease patients also showed content of docosahexaenoic acid, which increased lipid peroxidizability. In accordance, *N*^ε-(malondialdehyde)-lysine formation targeted important proteins for both glial and neuronal homeostasis such as neurofilament L, α -tubulin, glial fibrillary acidic protein, ubiquinol-cytochrome *c* reductase complex protein I, and the β chain of ATP synthase. These data support an important role for lipid peroxidation-derived protein modifications in Alzheimer disease pathogenesis.

* This work was supported by Spanish Ministry of Science and Technology Grant BFI2003-01287, Spanish Ministry of Health, Instituto de Salud Carlos III Grants FIS 02-0891 and 04-0355, the Amyotrophic Lateral Sclerosis Association, Generalitat de Catalunya Grant 2001ISGR00311 (to R. P. and M. P. O.), and Fondo de Investigaciones Sanitarias Grants 020004 and 03-006, Comisión Interministerial de Ciencia y Tecnología, Spain SAF-2001-4681E, and European Union project Brain Net Europe II (to I. F.). The costs of publication of this article were defrayed in part by the payment of page charges. This article must therefore be hereby marked "advertisement" in accordance with 18 U.S.C. Section 1734 solely to indicate this fact.

§ Both authors contributed equally to this work.

** To whom correspondence should be addressed: Departament de Ciències Mèdiques Bàsiques, Facultat de Medicina, Universitat de Lleida, c/Montserrat Roig, 2, E-25008 Lleida, Spain. Tel.: 34973702408; Fax: 34973702426; E-mail: manuel.portero@cmb.udl.es.

Oxidative stress-induced molecular alterations affect all sorts of biological molecules, including especially sensitive amino acid residues in proteins, such as tyrosine, methionine, arginine, proline, and lysine, among others (1). Brain aging is associated with changes increasing the risk of Alzheimer disease (AD).¹ A corollary of this fact is that AD shows an acceleration of those phenomena underlying aging. Accordingly, an increased amount of protein bound 2,4-dinitrophenylhydrazine (DNP)-reactive carbonyls, generated by protein oxidation are a common finding in brain samples from AD patients (2). All these works rely on the reaction of DNP with carbonyl groups. However, this assay has been criticized because of the possibility of artifacts (4). The direct measure of the concentration of structurally characterized products could overcome this fact and it may be used as a complement for assessing the effects of oxidative stress *in vivo*. Glutamic semialdehyde (GSA) derives from the metal-catalyzed oxidation of proline and arginine, whereas amino adipic semialdehyde (AASA) results from lysine oxidation (5). These products are among the main carbonyl products of metal-catalyzed oxidation of proteins (5), thus specific probes of oxidation of amino acids in protein. However, their presence and the factors affecting their concentrations in human brains are unknown to date.

The chemical pathways linking increased free radical efflux and protein structural modification also involve third-party molecules, which may give rise to increased DNP-reactive carbonyls in proteins (6). Particularly, carbohydrates, when reacting with free radicals generate highly reactive dicarbonyl compounds, such as glyoxal and methylglyoxal (7). In the cellular context, these may also be derived from glycolysis, triose phosphate metabolism, acetone metabolism (7), lipid peroxidation (8), and hypochlorite-mediated reactions (9). These compounds generate stable adducts reacting with lysine, arginine, and cysteine in proteins. *N*^ε-(Carboxyethyl)-lysine (CEL) and *N*^ε-

¹ The abbreviations used are: AD, Alzheimer disease; DNP, 2,4-dinitrophenylhydrazine; GSA, glutamic semialdehyde; AASA, amino adipic semialdehyde; CEL, *N*^ε-(carboxyethyl)-lysine; CML, *N*^ε-(carboxymethyl)-lysine; AGE, advanced glycation end products; PUFA, polyunsaturated fatty acids; MDAL, *N*^ε-malondialdehyde-lysine; A β , amyloid β -peptide; RAGE, receptor for advanced glycation end products; CHAPS, 3-[(cholamidopropyl)dimethylamino]-1-propanesulfonate; DTT, dithiothreitol; GC/MS, gas chromatography/mass spectrometry; UFA, unsaturated fatty acids; MUFA, monounsaturated fatty acids; ACL, average chain length; DHA, docosahexaenoic acid; MOPS, 3-(*N*-morpholino)propanesulfonic acid; MALDI-reTOF, matrix-assisted laser desorption/ionization reflectron time-of-flight.

(carboxymethyl)-lysine (CML) are two of these adducts, first described as advanced glycation end products (AGE), later named glycoxidation products and now recognized as mixed AGEs-advanced lipoxidation products. Despite that CML has been detected in AD lesions by immunohistochemical analyses (reviewed in Ref. 10), no chemical evidence have been reported for this product in AD samples or models. Polyunsaturated fatty acids (PUFA) are other third-party molecules. PUFA are molecules very susceptible to the oxidative action of free radicals (11), generating specific reactive aldehydes, such as malondialdehyde or 4-hydroxynonenal, among others (12). These aldehydes could react with proteins, generating also DNP-reactive moieties (6). The important PUFA content in brain and its high oxygen consumption support the possible significance of lipid peroxidation-derived processes in brain aging and AD pathogenesis (2). Analogously to the other modifications pointed out above, evidence for lipid peroxidation-derived protein damage in AD comprise immunohistochemistry (13). However, there is no chemical evidence for lipid peroxidative damage of proteins in AD, based on structurally identified compounds and supported by mass spectrometry.

Concerning the pathogenic role of these products, many recent studies of mechanisms underlying cellular dysfunction in Alzheimer disease have focused on amyloid β -peptide ($A\beta$). Persistent chronic inflammation appears to have a significant role in AD pathogenesis and evidence suggests that the sustained microglial response to $A\beta$ could play a role in this process (14). In AD brains, the most highly activated microglia is observed in close association with $A\beta$ plaques (15). In addition, many inflammatory mediators detected in AD brains are of microglial origin (14). *In vitro*, interaction of $A\beta$ with microglia has been shown to cause the induction of a range of inflammatory products, including proinflammatory cytokines, neurotoxic factors, reactive oxygen species, and complement pathway proteins (15, 16). Multiple $A\beta$ -binding protein or receptors have been identified on a number of different cell types, including microglia. They cover cell surface heparan proteoglycans and signal transduction receptors (17).

The receptor for advanced glycation end products (RAGE) is one of these cell surface $A\beta$ -binding proteins (18). RAGE is a member of the immunoglobulin superfamily of cell surface molecules whose expression is up-regulated at sites of diverse pathologies from atherosclerosis to AD (19). The generation of reactive oxygen species, an early event after ligation of the receptor, may be fundamental for many RAGE-induced changes in cellular properties. In the case of neurons, RAGE-induced cellular activation ultimately results in induction of programmed cell death (20).

In this work, we attempted to identify and quantify the amount of oxidation-derived modified amino acids in proteins from the frontal cerebral cortex of human brains with AD. Prior, we evaluated the distribution of these protein modifications by Western blot, the possible influence of sample preparation in DNP-based outcomes, and studied part of the biological response to these products by examining RAGE expression. Finally, given the importance of PUFA in lipid peroxidation, we also studied the fatty acid profile from these samples and the identification of major targets of lipoxidative damage in brain cortex.

MATERIALS AND METHODS

Human Brain Specimens and Reagents—Brain samples were obtained from the Institute of Neuropathology Brain bank following the guidelines of the local ethics committee. The brains of 8 patients with AD (four men and four women) and 5 age-matched controls (three women and two men) were obtained from 2 to 13 h after death, and were immediately prepared for morphological and biochemical studies. The agonal state was short with no evidence of acidosis or prolonged hy-

TABLE I
Summary of the main clinical and neuropathological findings in the present series

Alzheimer disease, stages C of amyloid- β A4 deposition, and stages V and VI of neurofibrillary degeneration (NFT) according to Braak and Braak (21) M: male, F: female.

Patient	Disease	Gender	Age	Duration of the disease	Post-mortem	Braak stages	
						Amyloid- β A4	NFT
			years	years	h		
1	Control	F	73		5.3		
2	Control	M	75		6		
3	Control	F	79		7		
4	Control	F	80		3.3		
5	Control	M	70		6		
6	AD	M	69	8	6	C	V
7	AD	F	82	13	10	C	V
8	AD	F	84	8	2	C	V
9	AD	F	86	8	10	C	V
10	AD	M	93	10	7.2	C	V
11	AD	M	71	6	13	C	VI
12	AD	M	72	7	6	C	VI
13	AD	F	72	8	5	C	VI

poxia. AD changes were categorized following the nomenclature of Braak and Braak (21). Stage C of amyloid A4 deposition implicates involvement of the whole neocortex, whereas stages V and VI of neurofibrillary degeneration indicate moderate and severe involvement of the neocortex. No additional vascular or degenerative anomalies were present in these cases. Age-matched controls did not show neuropathological anomalies, particularly considering the absence of amyloid deposits often considered as normal old-age changes. Frozen samples of the frontal cortex (area 8) were used for biochemical studies. Samples of control and diseased brains were processed in parallel. Summary of the main clinical and neuropathological aspects is shown in Table I. Unless otherwise specified, all reagents were from Aldrich or Sigma, of the highest purity available.

Distribution of Protein Modifications by Western Blotting and Derivatization of Proteins for Carbonyl Detection—Samples were homogenized in a buffer containing 180 mM KCl, 5 mM MOPS, 2 mM EDTA, 1 mM diethylenetriaminepentaacetic acid, and 1 μ M butylated hydroxyl toluene, 10 μ g/ml aprotinin, 1 mM phenylmethylsulfonyl fluoride, pH 7.3 (Potter-Elvehjem device, at 4 °C). After a brief centrifugation (500 \times g, 5 min) to pellet cellular debris, protein concentrations were measured in the supernatants using the Lowry assay (Bio-Rad).

Prior to electrophoresis, samples were derivatized with DNP as previously described (22). Briefly, to 15- μ l homogenates adjusted to 3.75 μ g/ μ l of protein, SDS was added to a final concentration of 6%, and after boiling for 3 min, 20 μ l of 10 mM DNP in 10% trifluoroacetic acid were added. After 7 min at room temperature, 20 μ l of a solution containing 2 M Tris base, 30% glycerol, and 15% β -mercaptoethanol were added for neutralization and sample preparation for loading onto SDS-PAGE gels. For sample clarification, prior to derivatization, chloroform (2:1, v/v) was added to an aliquot of the homogenates. Samples were then vortexed for 1 min and centrifuged at 13,000 \times g for 10 min. The proteins in the resulting supernatant were measured using the Bio-Rad method and equalized.

Immunodetection of Protein-bound 2,4-Dinitrophenylhydrazones, AGEs and CML—For immunodetection, after SDS-PAGE, proteins were transferred using a Mini Trans-Blot Transfer Cell (Bio-Rad) to polyvinylidene difluoride membranes (Immobilon-P, Millipore, Bedford, MA). Immunodetection was performed using as primary antibodies: a rabbit anti-DNP antiserum (1:4000, Dako, Carpinteria, CA); 6D12, a monoclonal anti-CML antibody (1:2000, Transgenic Inc., Kumamoto, Japan); and a polyclonal anti-AGE antiserum, raised against glyoxilic acid-treated keyhole limpet hemocyanin (1:2000). Peroxidase-coupled secondary antibodies were used from the Tropix chemiluminescence kit (Tropix Inc., Bedford, MA). Luminescence was recorded and quantified in Lumi-Imager equipment (Boehringer), using the Lumianalyst software. Control experiments showed that EDTA presence does not lead to generation of artifactual oxidation and that omission of the derivatization step, primary or secondary antibody addition produced blots with no detectable signal (data not shown).

Immunodetection of RAGE—A slightly modified protocol was used. Briefly, samples (0.2g) from diseased and control cases were homogenized in a glass homogenizer in 10 volumes of ice-cold lysis buffer (Hepes, pH 7.5, 250 mM sucrose, 10 mM KCl, 1.5 mM $MgCl_2$, 1 mM

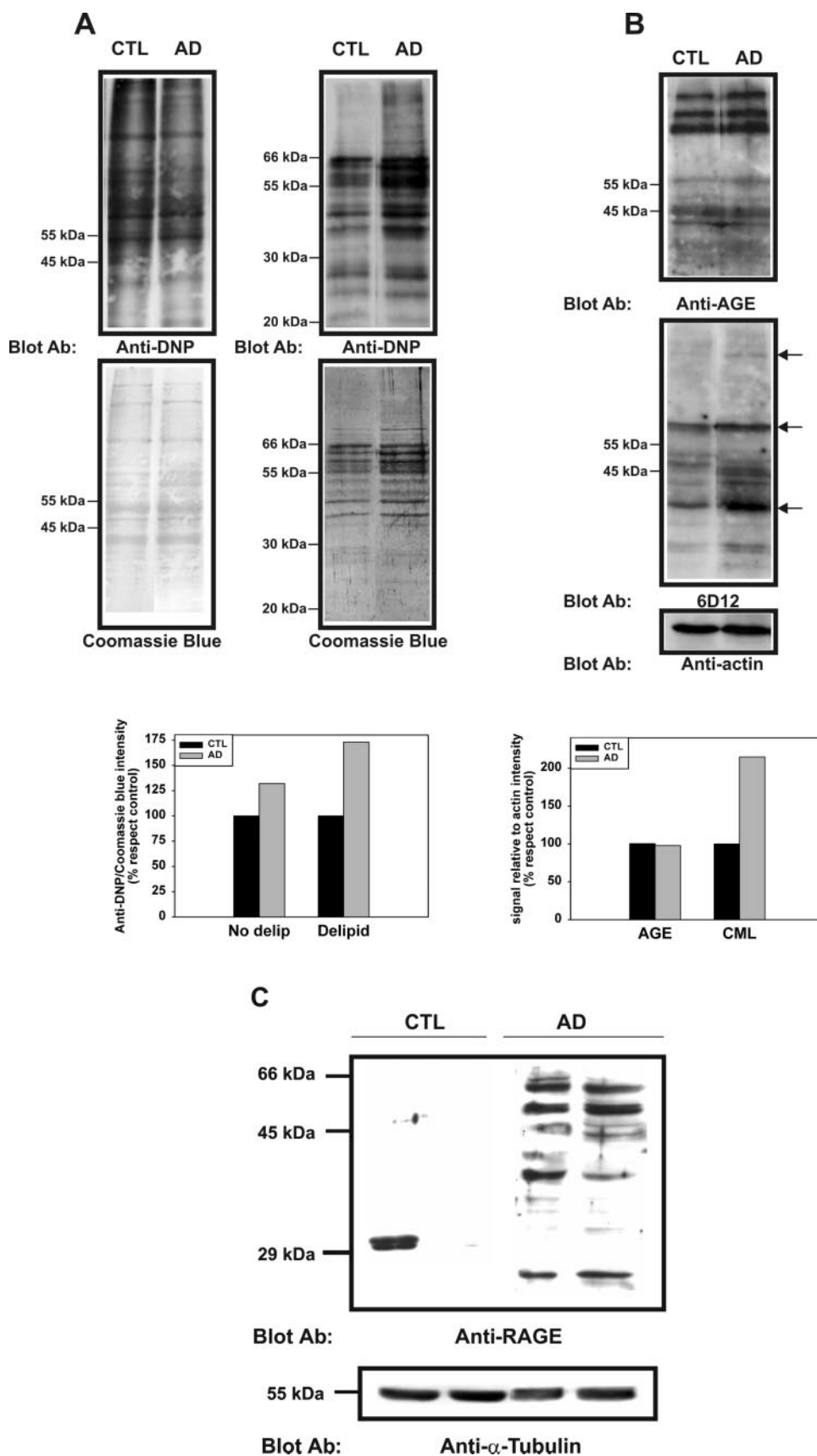


FIG. 1. AD induces differences in the distribution of protein oxidative modifications and in RAGE expression in homogenates from brain samples. Protein carbonyl groups, markers of protein oxidative damage, were derivatized with DNPH, and after their separation by SDS-PAGE, their amount was revealed by immunoblotting (A, left graph). After delipidation, differences between individual bands were more clear (A, right graph). Western blot analyses measured also AGE (B, upper blot) and CML (B, middle 6D12 blot) protein modifications. Arrows indicate bands noticeably different in AD samples. Right numbers of the blots indicate apparent molecular weight. The lower panels show the quantitation of these blots by densitometry. AD also induces differences in RAGE expression as shown by Western blot analyses of individual samples that revealed differences in distribution and amount of anti-RAGE immunoreactive bands (C shows representative blots from brain cortex of control individuals and AD patients).

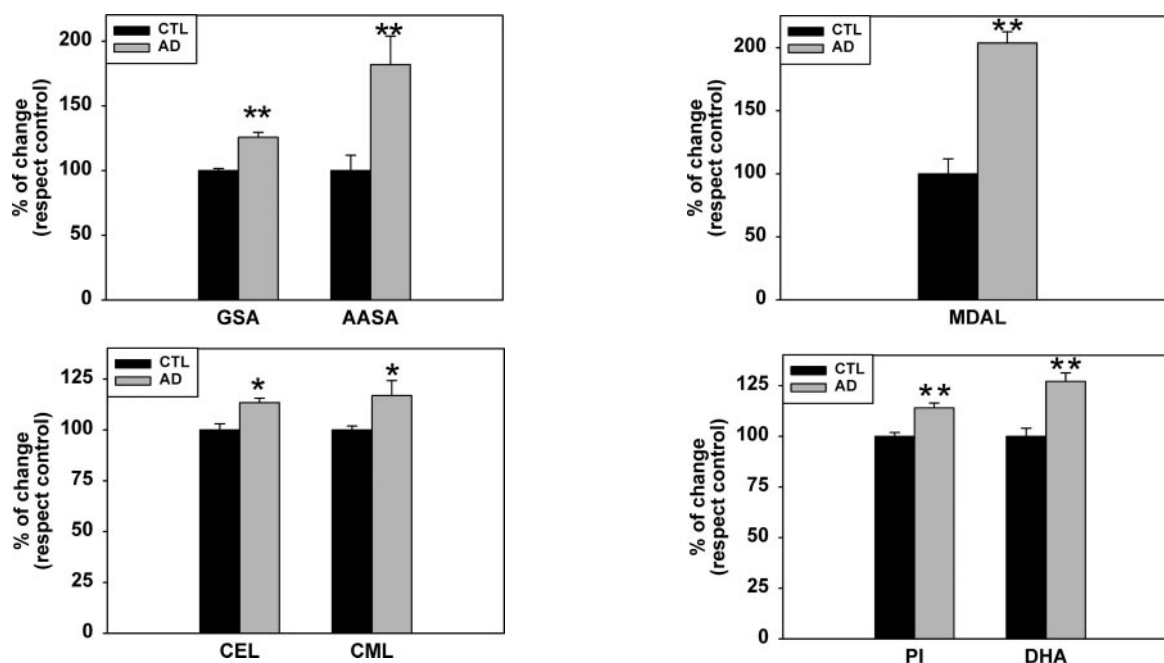


FIG. 2. Proteins from AD samples show significant increases in the amounts of GSA and AASA, markers of MCO (upper graph), and in the concentrations of CML and CEL, arising from glycoxidation and lipoxidation (lower graph). Values shown are % changes of mean \pm S.E. over values from control samples (GSA, $20,832 \pm 350$ $\mu\text{mol/mol}$ of lysine; AASA, 100 ± 12 $\mu\text{mol/mol}$ of lysine; CML, 497 ± 10 $\mu\text{mol/mol}$ of lysine; CEL, 462 ± 14 $\mu\text{mol/mol}$ of lysine). *, $p < 0.01$, and **, $p < 0.001$ respect to control group by Student's t test.

EDTA, 1 mM EGTA, 1 mM dithiothreitol (DTT), 10 $\mu\text{g/ml}$ aprotinin, 1 mM phenylmethylsulfonyl fluoride), and centrifuged at $5,000 \times g$ for 10 min at 4°C . Pellet fractions were discarded and protein concentrations of the supernatants were determined by the bicinchoninic acid method with bovine serum albumin as a standard.

Samples containing 50 μg of protein were loaded onto 10% SDS-PAGE gels. Proteins were separated by SDS-PAGE and electrophoretically transferred to nitrocellulose filters. After transfer, the filters were blocked by incubation with 5% nonfat dry milk in 100 mM Tris-buffered saline-Tween, containing 140 mM NaCl, 0.1% Tween 20, pH 7.4 (TBS-T), 1 h at room temperature. Then the filters were incubated overnight with TBS-T containing 3% bovine serum albumin and anti-RAGE antibody (Santa Cruz Biotechnology Inc., Santa Cruz, CA) at 1:100 dilution. Next, the filters were washed three times in TBS-T and incubated with TBS-T containing 5% skimmed milk and horseradish peroxidase-linked goat immunoglobulins (Dako) diluted 1:1000 for 45 min at room temperature. Filters were washed several times in TBS-T, and immunoreactivity was detected using an enhanced chemiluminescence Western blot detection system (Amersham Biosciences), followed by exposure to ECL HYPER film (Amersham Biosciences). Mouse monoclonal anti- α -tubulin at a dilution of 1:5000 was used to ensure equal loading of samples.

Two-dimensional Electrophoresis—Cortex samples were homogenized in a denaturation buffer (9 M urea, 4% CHAPS, 0.8% 3–11 IPG NL Buffer (Amersham Biosciences), 1% DTT and protein was quantified. An aliquot containing 50 μg of protein was adjusted to a final volume of 200 μl using rehydration buffer (8 M urea, 0.5% CHAPS, 0.5% 3–11 IPG NL Buffer, 18, 15 mM DTT, and 2% bromophenol blue) and applied overnight to 3–11 NL 11-cm IPG Strips (Amersham Biosciences). Isoelectric focusing was performed as follows: 500 V for 3 h, a linear gradient to 1000 V for 1 h, and finally 6000 V for 3 h in a Bio-Rad system. Strips were then incubated for 10 min in 37.5 mM Tris-HCl, pH 8.8, containing 6 M urea, 2% (w/v) SDS 20% (v/v) glycerol, and 0.5% DTT, and then re-equilibrated for 10 min in the same buffer except that DTT was replaced with 4.5% iodoacetamide. The equilibrated strips were loaded in a 11% 20-cm long SDS-PAGE gel and run as described in one-dimensional electrophoresis. Immunoblotting was performed as described above, using a Semidry transfer system and an anti-MDAL polyclonal antibody (Academy Biomedical Co., Houston, TX) as primary antibody (1:2000). For gel staining, a MS-modified silver staining method (Amersham Biosciences) was used as described by the manufacturer. For membrane staining, a silver staining method based on the

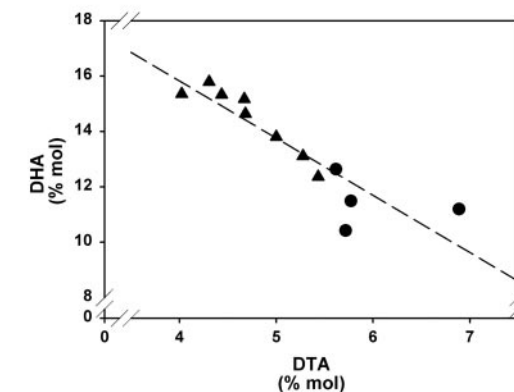


FIG. 3. Proteins from AD samples show significant increases in lipid peroxidation-derived damage, as shown by measurements of MDAL (upper graph), and this is associated with perceptual changes in peroxidizability index (PI) and DHA content (middle panel) and an inverse relationship between DHA and docosahexaenoic acid content (DTA) ($r = -0.89$; $p < 0.0001$, lower panel). Values shown are % changes of mean \pm S.E. over values from control samples (MDAL, 260 ± 31 $\mu\text{mol/mol}$ of lysine; DHA, $1,143 \pm 0.46\%$; peroxidizability index, 150.38 ± 2.82 **), $p < 0.001$ respect to control group by Student's t test. In the lower panel, triangles (▲) represent values from samples of AD patients and circles (●) represent values from control samples.

Gallyas intensifier was used according to previously described procedures (23).

Image Analysis—The gels (4 for each group) and polyvinylidene difluoride blots ($n = 5$) were scanned using a GS800 Calibrated Densitometer (Bio-Rad). PDQuest two-dimensional analysis software (Bio-Rad) was used for matching and analysis of silver-stained gels and membranes. The average mode of background subtraction was chosen to compare protein and MDAL immunoreactivity content between cortex samples from AD patients and control individuals. Normalized intensities of each protein spot from individual gels (or membranes) were compared between groups by the Student's t test.

Mass Spectrometry for Protein Identification—After excision from gel, proteins were reduced with 10 mM DTT and alkylated with 55 mM iodoacetamide. Enzymatic digestion was performed with trypsin (Promega, Madison, WI) following conventional procedures as described (24). After evaporation and redissolution in methanol/water (1:2 v/v), 1% acetic acid, digests were analyzed by matrix-assisted laser desorption/ionization reflectron time-of-flight (MALDI-reTOF MS).

The MALDI-reTOF MS analysis of the samples was performed using

a Voyager DE-PRO MALDI-reTOF mass spectrometer (Applied Biosystems, Foster City, CA). The instrument was run in reflectron mode with an average resolution of 12,000 full-width half-maximum at m/z 1500. A 5 mg/ml α -cyano-4-hydroxycinnamic solution was used as MALDI matrix. Spectra were externally calibrated using a standard peptide mixture consisting of angiotensin II, substance P, bombesin, and adrenocorticotrophic hormone. When the ions corresponding to known trypsin autolytic peptides (m/z 842.5100 and 2111.1046) were detected, a second automatic internal calibration of the spectra was performed using these ions as reference.

Data Base Search—The Protein Prospector software version 4.0.1 (University of California San Francisco, Mass Spectrometry Facility) was used to identify proteins from the peptide mass fingerprinting obtained from MALDI-reTOF MS. Swiss-Prot (European Bioinformatics Institute, Heidelberg, Germany) and GenBank™ (National Center for Biotechnology Information) data bases were used for the search.

Measurement of GSA, AASA, CML, CEL, and MDAL—GSA, AASA, CML, CEL, and MDAL concentrations in total proteins from cerebral cortex homogenates were measured by gas chromatography/mass spectrometry (GC/MS) as previously described (25). Samples containing 0.75–1 mg of protein were delipidated using chloroform/methanol (2:1, v/v), and proteins were precipitated by adding 10% trichloroacetic acid (final concentration) and subsequent centrifugation. Protein samples were reduced overnight with 500 mM NaBH₄ (final concentration) in 0.2 M borate buffer, pH 9.2, containing 1 drop of hexanol as an anti-foam reagent. Proteins were then reprecipitated by adding 1 ml of 20% trichloroacetic acid and subsequent centrifugation. The following isotopically labeled internal standards were then added: [²H₈]lysine (*d8*-Lys; CDN Isotopes); [²H₄]CML (*d4*-CML), [²H₄]CEL (*d4*-CEL), and [²H₈]MDAL (*d8*-MDAL), prepared as described (8, 26); and [²H₅]5-hydroxy-2-aminovaleic acid (for GSA quantization) and [²H₄]6-hydroxy-2-aminocaproic acid (for AASA quantization) prepared as described in Ref. 5. The samples were hydrolyzed at 155 °C for 30 min in 1 ml of 6 N HCl, and then dried *in vacuo*. The *N,O*-trifluoroacetyl methyl ester derivatives of the protein hydrolysate were prepared as previously described (5). GC/MS analyses were carried out on a Hewlett-Packard model 6890 gas chromatograph equipped with a 30-m HP-5MS capillary column (30 m × 0.25 mm × 0.25 μm) coupled to a Hewlett-Packard model 5973A mass selective detector (Agilent, Barcelona, Spain). The injection port was maintained at 275 °C; the temperature program was 5 min at 110 °C, then 2 °C/min to 150 °C, then 5 °C/min to 240 °C, then 25 °C/min to 300 °C, and finally hold at 300 °C for 5 min. Quantification was performed by external standardization using standard curves constructed from mixtures of deuterated and non-deuterated standards. Analytes were detected by selected ion-monitoring GC/MS. The ions used were: lysine and *d8*-lysine, m/z 180 and 187, respectively; 5-hydroxy-2-aminovaleic acid and *d5*-5-hydroxy-2-aminovaleic acid (stable derivatives of GSA), m/z 280 and 285, respectively; 6-hydroxy-2-aminocaproic acid and *d4*-6-hydroxy-2-aminocaproic acid (stable derivatives of AASA), m/z 294 and 298, respectively; CML and *d4*-CML, m/z 392 and 396, respectively; CEL and *d4*-CEL, m/z 379 and 383, respectively; and MDAL and *d8*-MDAL, m/z 474 and 482, respectively. The amounts of products were expressed as the ratio of micromole of glutamic semialdehyde, amino adipic semialdehyde, CML, CEL, or MDAL/mol of lysine.

Fatty Acid Analysis—Fatty acid analysis was performed as previously described (25). Total lipids from human brain homogenates were extracted with chloroform/methanol (2:1, v/v) in the presence of 0.01% butylated hydroxytoluene. The chloroform phase was evaporated under nitrogen, and the fatty acids were transesterified by incubation in 2.5 ml of 5% methanolic HCl for 90 min at 75 °C. The resulting fatty acid methyl esters were extracted by adding 2.5 ml of *n*-pentane and 1 ml of saturated NaCl solution. The *n*-pentane phase was separated, evaporated under nitrogen, redissolved in 75 μl of carbon disulfide, and 1 μl was used for GC/MS analysis. Separation was performed in a SP2330 capillary column (30 m × 0.25 mm × 0.20 μm) in a Hewlett-Packard 6890 Series II gas chromatograph (Agilent). A Hewlett-Packard 5973A mass spectrometer was used as detector in the electron-impact mode. The injection port was maintained at 220 °C, and the detector at 250 °C; the temperature program was 2 min at 100 °C, then 10 °C/min to 200 °C, then 5 °C/min to 240 °C, and finally hold at 240 °C for 10 min. Identification of fatty acid methyl esters was made by comparison with authentic standards and based on mass spectra. Results are expressed as mol %.

From fatty acid composition, the following indexes were calculated: saturated fatty acids = Σ % of saturated fatty acids; unsaturated fatty acids (UFA) = Σ % unsaturated fatty acids; monounsaturated fatty

TABLE II
Fatty acid composition and derived indexes in brain samples from AD patients and control individuals

Values shown are mean ± S.E. ACL, average chain length; SFA, saturated fatty acids; UFA, unsaturated fatty acids; PUFA *n*-6/*n*-3, polyunsaturated fatty acids *n*-6 or *n*-3 series; DBI, double bond index.

Fatty acid	Control	AD
14:0	0.59 ± 0.06	0.48 ± 0.02 ^a
16:0	16.60 ± 0.15	19.81 ± 0.66 ^a
16:1n-7	1.76 ± 0.11	1.19 ± 0.01 ^a
18:0	23.67 ± 0.35	21.50 ± 0.39 ^a
18:1n-9	26.78 ± 0.12	23.27 ± 0.77 ^a
18:2 <i>n</i> -6	0.66 ± 0.05	0.85 ± 0.10
18:3 <i>n</i> -3	0.12 ± 0.01	0.07 ± 0.003 ^a
20:0	1.97 ± 0.19	1.64 ± 0.16
20:1	0.13 ± 0.01	0.20 ± 0.009
20:2 <i>n</i> -6	0.26 ± 0.02	0.21 ± 0.01 ^a
20:3 <i>n</i> -6	0.76 ± 0.09	0.58 ± 0.02 ^a
20:4 <i>n</i> -6	6.91 ± 0.46	6.91 ± 0.42
22:4 <i>n</i> -6	5.99 ± 0.29	4.68 ± 0.19 ^a
22:5 <i>n</i> -6	0.52 ± 0.09	0.62 ± 0.02
22:5 <i>n</i> -3	0.10 ± 0.006	0.30 ± 0.03 ^a
24:0	0.20 ± 0.03	0.61 ± 0.07 ^a
24:1n-9	1.45 ± 0.15	2.46 ± 0.27 ^a
ACL	18.63 ± 0.02	18.74 ± 0.02
SFA	43.05 ± 0.11	44.06 ± 0.51
UFA	56.94 ± 0.11	55.93 ± 0.51
MUFA	30.14 ± 0.24	27.12 ± 0.74 ^a
PUFA	26.79 ± 0.33	28.80 ± 0.56
PUFA <i>n</i> -6	15.12 ± 0.45	13.88 ± 0.49
PUFA <i>n</i> -3	11.66 ± 0.46	14.92 ± 0.50 ^a
DBI	158.08 ± 1.78	169.55 ± 2.49 ^a

^a Indicates significant differences with control group as assessed by Student's *t* test ($p < 0.05$).

acids (MUFA) = Σ % of monoenoic fatty acids; polyunsaturated *n*-3 fatty acids (PUFAn-3) = Σ % of polyunsaturated fatty acids *n*-3 series; polyunsaturated *n*-6 fatty acids (PUFAn-6) = Σ % of polyunsaturated fatty acids *n*-6 series; average chain length = [(Σ % Total_{1,4} × 14) + ... + (Σ % total_{*n*} × *n*)]/100 (*n* = carbon atom number); peroxidizability index = [(Σ mol % monoenoic × 0.025) + (Σ mol % dienoic × 1) + (Σ mol % trienoic × 2) + (Σ mol % tetraenoic × 4) + (Σ mol % pentaenoic × 6) + (Σ mol % hexaenoic × 8)] (11).

Statistical analyses—All statistics were performed using the SPSS software (SPSS Inc., Chicago, IL). Differences between groups were analyzed by the Student's *t* tests. Correlations between variables were evaluated by the Pearson's statistic. The 0.05 level was selected as the point of minimal statistical significance in every comparison.

RESULTS

Western Blot Analyses of Brain Proteins Show Differences in DNP-reactive Carbonyls Depending on Sample Preparation and in RAGE Both Expression and Electrophoretic Mobility

The Western blot analyses of total homogenates did not show major differences in the distribution of oxidative damage (Fig. 1A). However, and stressing the importance of sample preparation for carbonyl analyses, after chloroform treatment several bands around 40 to 65 kDa showed increased oxidative damage in AD samples (Fig. 1A). To know which of these DNP-reactive carbonyls were related to glycooxidation or related reactions, we performed Western blots with different anti-AGE preparations. Staining with a polyclonal anti-AGE did not reveal any evident difference. Nonetheless, AD samples exhibited increased glycooxidative (6D12 antibody) damage, and the targets of these modifications showed diverse molecular masses, from 30 to 50 kDa (Fig. 1B). In accordance with increased AGE formation, immunoblotting for RAGE demonstrated three major bands at ~30, 50, and 60 kDa in AD cases, whereas as control specimens only showed one lower molecular weight band occasionally (Fig. 1C).

Proteins from Human Brain Cortex Present Structurally Characterized Oxidation Products and the Amount of These Modifications Increases with Alzheimer Disease

To offer a more accurate quantitative measurement of oxidation in brain proteins, we used isotope-dilution GC/MS. Proteins from human brain samples contained oxidation products resulting from metal-catalyzed oxidation, glycoxidation, and lipoxidation. An analysis of their distribution reveals that the more abundant products were those derived from metal-catalyzed oxidation, AASA and GSA (almost 95% of measured markers) (data not shown). GSA stood as the more frequent modification, with levels being 40-fold higher than those of AASA. The mean concentrations of both GSA and AASA were significantly higher ($p < 0.001$) in brain samples from AD patients than in control, age-matched individuals (Fig. 2). The mean concentrations of CEL and CML were also significantly higher ($p < 0.01$) in brain proteins from AD patients than in control individuals (Fig. 2). The concentration of MDAL, a lipoxidation product, was also significantly increased in samples from AD patients ($p < 0.001$; Fig. 3).

Changes in Fatty Acid Composition Associated with Alzheimer Disease Favor Lipoxidative Modification of Proteins

The analyses of fatty acid revealed significant differences associated with AD in brain samples, both in individual fatty acids and in global indexes (Table II). The 24:0 and 22:5, quantitatively minor fatty acids, exhibited 3-fold increases in their % content in AD samples. The highly peroxidizable docosahexaenoic acid (DHA) also showed a significant increase in its content ($p < 0.001$; Fig. 3) in these samples. Interestingly, DHA levels were inversely correlated with docosatetraenoic acid levels ($r = -0.89$; $p < 0.0001$; Fig. 3). AD samples showed almost half of the % contents of 18:3 and 16:1, compared with the control samples. With reference to the derived indexes, AD samples showed significant decreases for monounsaturated fatty acids, with subsequent increases in the content of PUFA of the $n-3$ family. This resulted in a significantly increased double bond (Table I) and peroxidizability indexes (Fig. 3).

Different Kinds of Protein Oxidative Damage Are Correlated

Association between Changes in Fatty Acid-derived Indexes and Protein Oxidative Damage—After quantitation of protein oxidation indexes and fatty acid analyses, several significant correlations were observed (Fig. 4). GSA levels correlated significantly with AASA ($r = 0.86$; $p < 0.0001$), with CML ($r = 0.73$; $p < 0.007$), and with MDAL ($r = 0.79$; $p < 0.002$). This suggests that protein carbonyl formation is associated also to glycoxidative and lipoxidative modifications. Furthermore, GSA concentrations correlated directly to peroxidizability indexes ($r = 0.69$; $p < 0.01$) (Fig. 4), suggesting an association between lipid peroxidizability and metal-catalyzed modification. Interestingly, levels of CML, a mixed glyco and lipoxidation product, are directly correlated with arachidonic acid levels ($r = 0.62$; $p < 0.03$), suggesting that in these samples, lipid peroxidation could be a major source of CML.

MDAL Formation Targets Several Structural Proteins and Enzymes with Key Roles in Cellular Homeostasis—After two-dimensional electrophoresis and Western blot with an anti-MDAL antibody, the reactivity of several spots already present in samples from control individuals was increased in brain cortex proteins from AD patients (Fig. 5). Nonetheless, some novel spots also appeared in Western blots of these later. Several structural proteins, mitochondrial and cytosolic enzymes, as well as other proteins, were identified after peptide finger-

printing by MALDI (Table III). Among those, several showed significant increases in MDAL immunostaining in AD samples such as neurofilament protein L (3-fold), α -tubulin (9-fold), glial fibrillary acidic protein (8-fold), γ -enolase (2-fold), ubiquinol-cytochrome *c* reductase complex core protein I (4-fold), and β chain of ATP synthase (4-fold).

DISCUSSION

Our data support the presence of protein oxidation-derived markers in brain samples from aged individuals and AD patients by mass spectrometric evidence. In the present work, brain proteins have been analyzed, and we found that the contents of specific carbonyl AASA and GSA in AD samples were significantly increased. This fact could be related to a mitochondrial dysfunction that would promote the leakage of reactive oxygen species, subsequently increasing protein oxidative damage (27). Furthermore, the results agree with those previously suggesting that increased oxidative damage occurs in AD (2, 28), although in these reports it affects specifically some other brain regions such as temporal inferior cortex (29) or parietal lobe cortex (28). The increase in carbonyl concentrations in these reports is lower than that found here for AASA, but not for GSA. Our mass spectrometric data also demonstrate an increase in glycoxidative damage in AD. As glycolytic intermediates generate CML and CEL (7), these findings agree with the key role of glycolysis in brain. Vulnerable neurons may have increased dicarbonyl products and/or decreased turnover of modified proteins (30). These data fit with increased carbonyl reductase, alcohol dehydrogenase (31), and pentose-phosphate pathway activities (32) in brains from AD patients. In addition, recent data stress the potential importance of glyoxalase I, an enzyme against reactive dicarbonyls, as a risk factor in AD pathogenesis (33). Coexistence of the RAGE overexpression with AGE may be a more pathogenically relevant finding than AGE alone. Increased RAGE expression in AD samples suggests a pathogenic role for this multiligand receptor. In some control individuals, anti-RAGE immunoreactivity was not evident or it was limited to a very low molecular weight that may be related to the Δ^8 -RAGE, a novel secreted splice variant of RAGE, recently identified in brain astrocytes and peripheral blood mononuclear cells (34). In clear contrast, AD samples exhibited a marked increase in immunoreactivity as well as in the molecular heterogeneity of the immunoreactive forms. These may belong to full-length RAGE (55 kDa) and to N-terminal RAGE (35 kDa), already identified in human brain tissue (35). The pathophysiological relevance of these findings is unknown but it is proposed that RAGE overexpression may reflect different responses to increased AGE or A β concentrations. Thus, as C-truncated RAGE forms are cytoprotective for endothelial cells (36) its overexpression in AD would constitute a defensive response. In contrast, expression of full-length RAGE could contribute to the acceleration of neuronal damage throughout activation of inflammatory responses and/or the accumulation of A β in brain parenchyma (37).

Lipid peroxidation-derived protein damage was also evidenced by GC/MS. MDAL appears to be the more sensible marker, as it increases almost 2-fold in samples from AD patients. This agrees with previous reports, stating immunohistochemical evidence for pronounced protein modification by 4-hydroxynonenal (38) in correlation with the severity of the disease (39). In a close relationship, we found that AD samples exhibit differences in fatty acid content. Thus, increased lipid peroxidizability index and DHA content sustain increased lipid peroxidation. It is known that A β induces hippocampal neuronal death by a mechanism that requires lipid peroxidation (39). Disturbances in the metabolism and transport of essential fatty acids may explain the observed changes (40), but they could

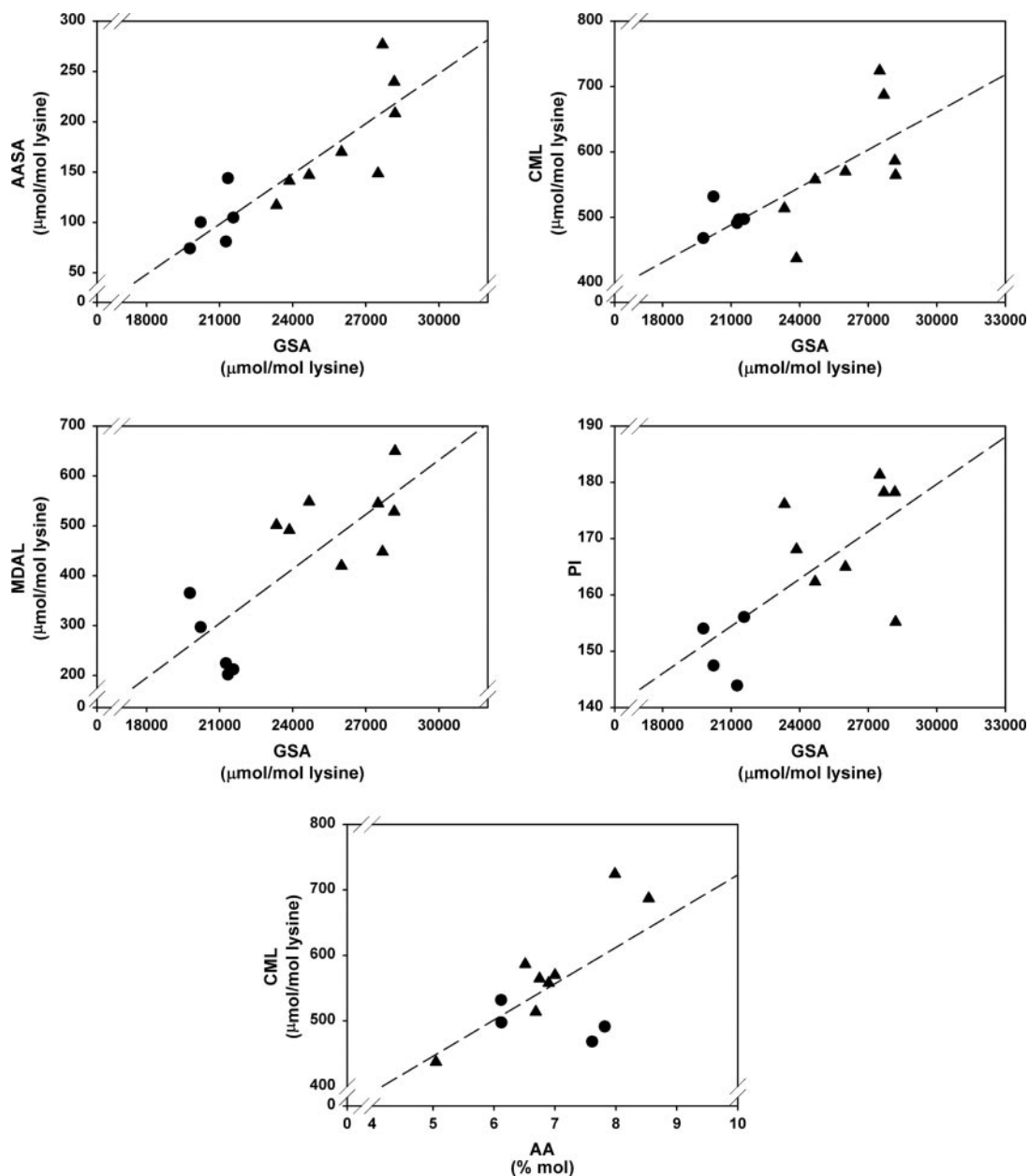


FIG. 4. **Protein oxidation indexes are strongly correlated.** Indexes of protein carbonyl GSA and AASA are strongly correlated (*upper panel, left*; $r = 0.86$; $p < 0.0001$). Protein oxidative damage is correlated with protein glycoxidative damage (*upper panel, right*; $r = 0.73$; $p < 0.007$) and protein lipoxidative damage (*middle panel, left*; $r = 0.79$; $p < 0.002$). Lipid composition also influences protein oxidative damage (*middle panel, right*; $r = 0.69$; $p < 0.01$) and protein glycoxidative modification (*lower panel*; $r = 0.62$; $p < 0.04$). AA: arachidonic acid; triangles (\blacktriangle) represent values from samples of AD patients and circles (\bullet) represent values from control samples.

also originate from a defensive response, because of the neuroprotective role of DHA in several experimental models (41). However, this may be a double-edged sword, as DHA is a highly peroxidizable fatty acid.

We also identified major targets of lipoxidative modification by using an anti-MDAL antibody in combination with two-dimensional electrophoresis and MALDI peptide fingerprinting. The results demonstrated the modification of several proteins, some already known to be modified by anti-DNP immunoreactive compounds (2, 42) and some other novel. As discussed above, DNP reactivity alone does not discriminate between sources of oxidative damage. Therefore, it could be proposed that lipoxidation chemistry contributes significantly to carbonyl formation measurable by DNP reactivity. It could be also hypothesized that several types of oxidative damage simultaneously modify these proteins. A number of cytoskel-

etal proteins were identified as targets of MDAL formation, including NF-L, whose changes are involved in a murine model of age-dependent learning and memory deficits (43), β -tubulin and, in a lower extent α -tubulin. Prior studies demonstrated aberrant modifications of β -tubulin in AD samples (44). The electrophoretic motility pattern of glial fibrillary acidic protein in AD samples, another target of MDAL formation, is complex because of the presence of different modification and degradation forms (45). MDAL also modified several enzymes, some already known to be carbonylated in AD patients, such as creatine kinase BB, glutamine synthase, ubiquitin C-terminal hydrolase L-1, and γ -enolase (42). We also identified neuronal specific γ -enolase, which interconverts 2-phosphoglycerate to phosphoenolpyruvate in glycolysis. Previous works identified α -enolase and γ -enolase as specifically oxidized/nitrated in AD brain (42). Abnormalities in tissue bioenergetics have been

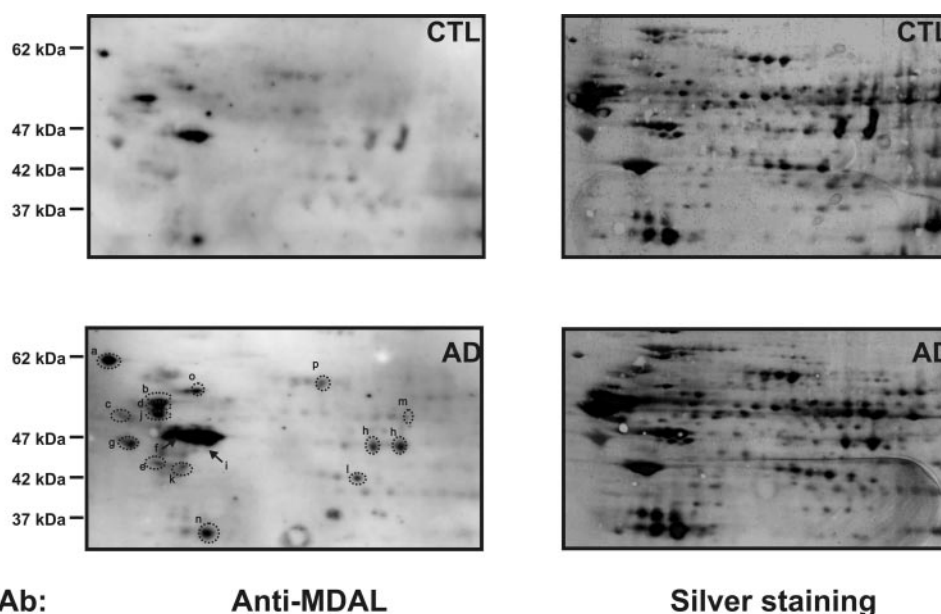


FIG. 5. **Brain cortex protein lipoxidative modifications in AD patients and a control population.** Identification of major targets. Brain cortex proteins were separated by two-dimensional electrophoresis and anti-MDAL Western blot was performed. Silver stain of membranes is also shown. Major damaged proteins from control and AD samples were identified by mass spectrometry (Table III).

TABLE III
Identification of major targets of lipoxidative damage in brain cortex

Spot ^a	Protein	<i>M_r</i> / <i>P</i> I	Peptides identified	Specific lipoxidation ^b	Accession number
				% control	
Cytoskeletal proteins					
a	Neurofilament triplet L	61777/4.7	21	350 ± 60	P07196
b	Vimentin	53686/5.1	36	NS	P08670
c	β-Tubulin 2	49831/5.8	19	187 ± 30	P05217
d	α-Tubulin 1	50151/5.0	15	958 ± 123	P05209
	α-Tubulin 4	49924/5.0			P05215
	α-Tubulin 6	49898/5.0			Q9BQE3
e	β-Actin	41738/5.3	13	NS	P02570
	γ-Actin	41793/5.3			P02571
f	Glial fibrillary acidic protein	49881/5.4	18	817 ± 42	P14136
Metabolism/Energy production					
g	γ-Enolase	47269/4.9	8	257 ± 37	P09104
h	α-Enolase	47169/7.0	15	NS	P06733
i	Ubiquinol-cytochrome <i>c</i> reductase complex core protein I	52619/6.0	15	429 ± 55	P31930
j	ATP synthase (β chain)	56560/5.3	19	412 ± 38	P06576
k	Creatine kinase, B chain (B-CK)	42645/5.3	15	153 ± 34	P12277
l	Glutamine synthetase	42065/6.4	14	144 ± 22	P15104
m	Glutamate dehydrogenase 1	61398/7.7	16	NS	P00367
Other					
n	Guanine nucleotide-binding protein G(I)/G(S)/G(T) β Subunit 1 or 2	37377/5.6	7	NS	P04901
	60-kDa heat shock protein	61055/5.7	14	134 ± 56	P10809
o	Dihydropyrimidinase-related protein-2 (DRP-2)	62294/6.0	18	NS	Q16555

^a Spot letter refers to two-dimensional gels obtained from brain cortex samples (Fig. 1).

^b For each protein, individual anti-MDAL immunostain/protein values (obtained from each of four AD and four control samples) were averaged and expressed as percentage of control ± S.E. ($p < 0.05$ between control and AD samples by Student's *t* test).

^c NS, nonsignificant differences.

previously linked to AD (46). In this line, a number of mitochondrial respiratory enzymes, with key roles in energy homeostasis were also targets of MDAL formation. Among these, ubiquinol-cytochrome *c* reductase complex core protein I is a major component of the mitochondrial oxidative phosphorylation complex III. ATP synthase (β chain) showed increased MDAL formation. Recent data point out that some ATP synthase chains accumulate in cytosol of degenerating neurons, in

some cases in a tight association with τ aggregates (47). Creatine kinase is also modified in brain from AD patients and experimental models (2, 42). The fact that vitamin E inhibits the AD-associated loss of activity of creatine kinase, strongly suggests a role for lipid peroxidation in this failure, further implicating the protein lipoxidative modification (13, 48). Glutamate synthase activity, with a key role in elimination of free ammonia in brain, is also decreased by AD, especially in glia

close to the affected areas (49). Glutamate synthase interacts with β A, enhancing its prooxidant properties and leading to lipid peroxidation (50), potentially explaining MDAL formation in this protein. In accordance with disturbances in glutamate metabolism as mediators in AD pathogenesis, another enzyme related to this neurotransmitter, glutamate dehydrogenase, was also modified with MDAL in AD samples. Other proteins, such as HSP60 and DRP2, were also identified as targets of MDAL formation. Our results, as well as others (42), suggest a pathogenic role for lipoxidative damage, affecting mitochondrial homeostasis and axon and neurite wiring.

Collectively, the results presented here support a role for both protein oxidative damage and changes in fatty acid composition in AD pathogenesis, with possible implications of RAGE. This would lead to disturbances in cytoskeleton and energy production, which ultimately would contribute to the generation of neurofibrillary tangles with the participation of lipid peroxidation.

Acknowledgments—We are deeply indebted to Dr. Jesus Requena (Universidad de Santiago de Compostela, Spain) from providing GSA and AASA standards and thoughtful comments. We also thank the team of Dr. Joaquin Abian (Structural and Biological Mass Spectrometry Unit, IDIBAPS, Barcelona, Spain) for MALDI services.

REFERENCES

- Amici, A., Levine, R. L., Tsai, L., and Stadtman, E. R. (1988) *J. Biol. Chem.* **365**, 3341–3346
- Aksenov, M. Y., Aksenova, M. V., Butterfield, D. A., Geddes, J. W., and Markesbery, W. R. (2001) *Neuroscience* **103**, 373–383
- Smith, C. D., Carney, J. M., Starke-Reed, P. E., Oliver, C. N., Stadtman, E. R., Floyd, R. A., and Markesbery, W. R. (1991) *Proc. Natl. Acad. Sci. U. S. A.* **88**, 10540–10543
- Cao, G., and Cutler, R. G. (1995) *Arch. Biochem. Biophys.* **320**, 106–114
- Requena, J. R., Chao, C. C., Levine, R. L., and Stadtman, E. R. (2001) *Proc. Natl. Acad. Sci. U. S. A.* **98**, 69–74
- Berlett, B. S., and Stadtman, E. R. (1997) *J. Biol. Chem.* **272**, 20313–20316
- Thornalley, P. J., Langborg, A., and Minhas, H. S. (1999) *Biochem. J.* **344**, 109–116
- Fu, M. X., Requena, J. R., Jenkins, A. J., Lyons, T. J., Baynes, J. W., and Thorpe, S. R. (1996) *J. Biol. Chem.* **271**, 9982–9986
- Anderson, M. M., Requena, J. R., Crowley, J. R., Thorpe, S. R., and Heinecke, J. W. (1999) *J. Clin. Invest.* **104**, 103–113
- Kikuchi, S., Shinpo, K., Takeuchi, M., Yamagishi, S., Makita, Z., Sasaki, N., and Tashiro, K. (2003) *Brain Res. Rev.* **41**, 306–323
- Cosgrove, J. P., Church, D. F., and Pryor, W. A. (1987) *Lipids* **22**, 299–304
- Esterbauer, H., Schaur, R. J., and Zollner, H. (1991) *Free Radic. Biol. Med.* **11**, 81–128
- Butterfield, D. A., Castegna, A., Lauderback, C. M., and Drake, J. (2002) *Neurobiol. Aging* **23**, 655–664
- Akiyama, H. S., Barger, S., Barnum, S., Bradt, B., Bauer, J., Cole, G. M., Cooper, N. R., Eikelenboom, P., Emmerling, M., Fiebich, B. L., Finch, C. E., Frautschy, S., Griffin, W. S., Hampel, H., Hull, M., Landreth, G., Lue, L., Mrak, R., Mackenzie, I. R., McGreer, P. L., O'Banion, M. K., Pachter, J., Pasinetti, G., Plata-Salman, C., Rogers, J., Rydel, R., Shen, Y., Streit, W., Strohmeyer, R., Tooyoma, I., Van Muiswinckel, F. L., Veerhuis, R., Walker, D., Webster, S., Wegrynkiak, B., Wenk, G., and Wysscoray, T. (2000) *Neurobiol. Aging* **21**, 383–421
- Itagaki, S., McGreer, P. L., Akiyama, H., Zhu, S., and Selkoe, D. (1989) *J. Neuroimmunol.* **24**, 173–182
- Haga, S., Ikeda, K., Sato, M., and Ishii, T. (1993) *Brain Res.* **601**, 88–94
- Yaar, M., Zhai, S., Pilch, P. F., Doyle, S. M., Eisenhauer, P. B., Fine, R. E., and Gilchrist, B. A. (1999) *J. Clin. Invest.* **100**, 2333–2340
- Brett, J., Schmidt, A. M., Yan, S. D., Zou, Y. S., Weidman, E., Pinski, D., Nowygrod, R., Neeper, M., Przysiecki, C., and Shaw, A. (1993) *Am. J. Pathol.* **143**, 1699–1712
- Schmidt, A. M., Yan, S. D., Wautier, J. L., and Stern, D. M. (1999) *Circ. Res.* **84**, 489–497
- Schmidt, A. M., Yan, S. D., Yan, S. F., and Stern, D. M. (2000) *Biochim. Biophys. Acta* **1498**, 99–111
- Braak, H., and Braak, E. (1999) *Cerebral Cortex: Neurodegenerative and Age-related Changes in Structure and Function of the Cerebral Cortex*, Vol. 14, Kluwer Academic/Plenum Press, NY
- Portero-Otin, M., Pamplona, R., Ruiz, M. C., Cabisco, E., Prat, J., and Bellmunt, M. J. (1999) *Diabetes* **48**, 2215–2220
- Sorensen, B. K., Hojrup, P., Ostergard, E., Jorgensen, C. S., Enghild, J., Ryder, L. R., and Houen, G. (2002) *Anal. Biochem.* **304**, 33–41
- Forne, I., Carrascal, M., Martinez-Lostao, L., Abian, J., Rodriguez-Sanchez, J. L., and Juarez, C. (2003) *J. Biol. Chem.* **278**, 50641–50644
- Pamplona, R., Portero-Otin, M., Requena, J., Gredilla, R., and Barja, G. (2002) *Mech. Ageing Dev.* **123**, 1437–1446
- Requena, J. R., Fu, M. X., Ahmed, M. U., Jenkins, A. J., Lyons, T. J., Baynes, J. W., and Thorpe, S. R. (1997) *Biochem. J.* **322**, 317–325
- Lustbader, J. W., Cirilli, M., Lin, C., Xu, H. W., Takuma, K., Wang, N., Caspersen, C., Chen, X., Pollak, S., Chaney, M., Trinchese, F., Liu, S., Gunn-Moore, F., Lue, L. F., Walker, G., Kuppasamy, P., Zewier, Z. L., Arancio, O., Stern, D., Yan, S. S., and Wu, H. (2004) *Science* **304**, 448–452
- Lyras, L., Cairns, N. J., Jenner, A., Jenner, P., and Halliwell, B. (1997) *J. Neurochem.* **68**, 2061–2069
- Bogdanovic, N., Zilmer, M., Zilmer, K., Rehema, A., and Karelson, E. (2001) *Dement. Geriatr. Cogn. Dis.* **12**, 364–371
- Munch, G., Shepherd, C. E., McCann, H., Brooks, W. S., Kwok, J. B., Arendt, T., Hallupp, M., Schofield, P., Martins, R. N., and Halliday, G. M. (2002) *Neuroreport* **13**, 601–604
- Balcz, B., Kirchner, L., Cairns, N., Fountoulakis, M., and Lubec, G. (2001) *J. Neural. Trans. Suppl.* **61**, 193–201
- Palmer, A. M. (1999) *J. Neural. Transm.* **106**, 317–328
- Chen, F., Wollmer, M. A., Hoernldi, F., Munich, G., Kuhla, B., Rogava, E. I., Tsolaki, M., Papassotiropoulos, A., and Gota, J. (2004) *Proc. Natl. Acad. Sci. U. S. A.* **101**, 7687–7692
- Park, I. H., Yeon, S. I., Youn, J. H., Choi, J. E., Sasaki, N., Choi, I. H., and Shin, J. S. (2004) *Mol. Immunol.* **40**, 1203–1211
- Sasaki, N., Toki, S., Chowei, H., Saito, T., Nakano, N., Hayashi, Y., Takeuchi, M., and Makita, Z. (2001) *Brain Res.* **888**, 256–262
- Yonekura, H., Yamamoto, Y., Sakurai, S., Petrova, R. G., Abedin, M. J., Li, H., Yasui, K., Takeuchi, M., Makita, Z., Takasawa, S., Okamoto, H., Watanabe, T., and Yamamoto, H. (2003) *Biochem. J.* **370**, 1097–1109
- Yan, S. D., Chen, X., Fu, J., Chen, M., Zhu, H., Roher, A., Slattery, T., Zhao, L., Nagashima, M., Morsler, J., Mighele, A., Nawroth, P., Stern, D., and Schmidt, A. M. (1996) *Nature* **382**, 685–691
- Montine T. J., Markesbery, W. R., Zackert, W., Sanchez, S. T., Roberts, L. J., and Morrow, J. D. (1999) *Am. J. Pathol.* **155**, 863–868
- Mark, R. J., Pang, Z., Geddes, J. W., Uchida, K., and Mattson, M. P. (1997) *J. Neurosci.* **17**, 1046–1054
- Rapoport, S. I., Chang, M. C., and Spector, A. A. (2001) *J. Lipid Res.* **42**, 678–685
- Barcelo-Coblijn, G., Hoguey, E., Kitajka, K., Puskas, L. G., Zvara, A., Hackler, L., Nyakas, C., Penke, Z., and Farkas, T. (2003) *Proc. Natl. Acad. Sci. U. S. A.* **100**, 11321–11326
- Castegna, A., Aksenov, M., Aksenova, M., Thongbookerd, V., Klein, J. B., Pierce, W. M., Booze, R., Markesbery, W. R., and Butterfield, D. A. (2002) *J. Neurochem.* **82**, 1524–1532
- Poon, H. F., Castegna, A., Farr, S. A., Thongbookerd, V., Lynn, B. C., Banks, W. A., Morley, J. E., Klein, J. B., and Butterfield, D. A. (2004) *Neuroscience* **126**, 915–926
- David, S., Shoemaker, M., and Haley, B. E. (1998) *Brain Res. Mol. Brain Res.* **54**, 276–287
- Porchet, R., Probst, A., Bouras, C., Drabero, E., Draber, P., and Riederer, B. M. (2003) *Proteomics* **3**, 1476–1485
- Shoffner, J. M. (1997) *Neurogenetics* **1**, 13–19
- Sergeant, N., Watzel, A., Galvan-Valencia, M., Ghestem, A., David, J. P., Lemoine, J., Sautiere, P. E., Dachary, J., Mazat, J. P., Michalski, J. C., Velours, J., Mena-Lopez, R., and Delacourte, A. (2003) *Neuroscience* **117**, 293–303
- Yatin, S. M., Aksenov, M., and Butterfield, D. A. (1999) *Neurochem. Res.* **24**, 427–435
- Robinson, S. R. (2000) *Neurochem. Int.* **36**, 471–482
- Oyama, R., Yamamoto, H., and Titan, K. (2000) *Biochim. Biophys. Acta* **1479**, 91–102

Proteins in Human Brain Cortex Are Modified by Oxidation, Glycooxidation, and Lipoxidation: EFFECTS OF ALZHEIMER DISEASE AND IDENTIFICATION OF LIPOXIDATION TARGETS

Reinald Pamplona, Esther Dalfó, Victòria Ayala, Maria Josep Bellmunt, Joan Prat, Isidre Ferrer and Manuel Portero-Otín

J. Biol. Chem. 2005, 280:21522-21530.

doi: 10.1074/jbc.M502255200 originally published online March 29, 2005

Access the most updated version of this article at doi: [10.1074/jbc.M502255200](https://doi.org/10.1074/jbc.M502255200)

Alerts:

- [When this article is cited](#)
- [When a correction for this article is posted](#)

[Click here](#) to choose from all of JBC's e-mail alerts

This article cites 49 references, 14 of which can be accessed free at <http://www.jbc.org/content/280/22/21522.full.html#ref-list-1>